Fabrication of porous biopolymer substrates for cell growth by UV laser: the role of pulse duration

Marta Castillejo*, Esther Rebollar, Mohamed Oujja, Mikel Sanz

Instituto de Química Física Rocasolano, CSIC, Serrano 119, 28006 Madrid, Spain

and

Alexandros Selimis, Maria Sigletou[1], Stelios Psycharakis, Anthi Ranella, Costas Fotakis[1]

Institute of Electronic Structure and Laser, Foundation for Research and Technology-Hellas, P.O. Box 1527, 71110 Heraklion, Crete, Greece

[1]Also at the *Physics Department, University of Crete, Heraklion, Greece*

*Email: marta.castillejo@iqfr.csic.es

Abstract

Ultraviolet laser irradiation using pulses with duration from the nanosecond to the femtosecond range was investigated aiming at the generation of a foam layer on films of the biopolymers chitosan, starch and their blend. We report on the morphological characteristics of the foams obtained upon irradiation and on the accompanying laser induced photochemistry, assessed by on line monitoring of the laser induced fluorescence. We identify the laser conditions (pulse duration) at which foaming is produced and discuss the obtained results in reference to the material properties, particularly extinction coefficient and thermal parameters. This article also reports on successful cell culture on the laser induced foam structure generated in chitosan, as an illustrative example of the possibility of broader use of laser induced biopolymer foaming structures in biology.

Keywords: Laser foaming, biopolymers, chitosan, starch, cell growth

1. Introduction

Biopolymers hold promise to become the fundamental building blocks for organic photonics and electronics; they constitute important sources of novel functional materials and advantageous alternatives to synthetic polymers in biomedical applications, i.e. for the fabrication of implants and controlled drug delivery systems, and more recently to replace conventional polymers in packaging, coatings, disposable products, fibres and films.

Biopolymer foams and microstructures, using collagen, gelatine, chitosan, starch and other biomaterials, are currently investigated as 2D and 3D scaffolds for cell culture. A variety of processing techniques, including stamping, stereo lithography, two-photon polymerization, electrospinning, polymer demixing and stencil [1-7], have been applied in order to control relevant properties such as pore size and distribution, interconnectivity, adequate surface chemistry, etc. Common simple, low-cost tools based on standard bioengineering micro-fabrication techniques, such as micro-contact printing or nanoimprint lithography, are prone with difficulties when dealing with biomaterials due to their typical non biocompatibility [3]. Alternative approaches in high-resolution patterning of biopolymers are searched for and, in particular, laser-based methods, already used for porous scaffold fabrication on various materials [8-10], are good candidate tools, as they afford the sought versatility and reliability [1,11-16].

2D scaffolds for cell culture are currently prepared by structuring the surface of polymers by some of the methods mentioned above, based on the fact that the topography, together with chemical composition, have influence on cell adhesion and proliferation. In the literature, different types on nano- and microstructures have been reported, such as grooves, ripples, islands, pillars, particles, dots and fibrillar networks [2-5,11-14,16-19]. Recently, superficial laser foaming on films of biopolymers such as

collagen and gelatine has been reported, a phenomenon that is induced by applying single pulses in the nanosecond (ns) to femtosecond (fs) domains [4,11-14,16-19]. The fast temperature rise causes a transient acoustic wave that contains both compressive and tensile components due to conservation of momentum. The compressive pressure wave within the dense material is followed by the tensile wave which is ultimately responsible for fast nucleation and bubble growth. It has been referred that these foam structures are good runners for fabrication of cell culture substrates, since, given the open interconnected pore structure, they exhibit increased availability of adhesion sites combined with permeability to fluids. Therefore, the absence in the literature of any report concerning cell culture on the laser induced foam structures on biopolymers is rather surprising. Indeed, such structures do not survive under the essential cell culture procedures based in incubation at 37 °C in water solution, as they collapse as soon as the solution, containing the nutritional ingredients essential for the cells life, is added to the laser-irradiated films. The reason for this behaviour is far from being obvious and laser induced photochemical changes should definitely be taken into account for its elucidation.

This work aims at a better understanding of the laser biopolymer interaction mechanisms, at an improved control of the microfoams and at the testing of the foamed material for developing 2D scaffolds for cell growth. Surface foaming was induced on chitosan, starch and their blend (self-standing films and films casted on quartz plates) by UV laser irradiation with pulse durations ranging from ns to fs. Chitosan is an aminopolysaccharide, the deacetylated derivative of chitin, which is the second most naturally occurring biopolymer after cellulose. This biopolymer offers a combination of properties uniquely suited for biofabrication, as its backbone provides sites that can be employed for the assembly of proteins, nucleic acids, and virus particles [20,21]. On the

other hand, starch is a polysaccharide, which in its native state from plants, contains about 30% amylose, 70% amylopectine and less than 1% lipids and proteins [22]. The tensile strength and the flexibility of starch films can be improved by incorporation of chitosan [23-25], and blends of these two biopolymers have been studied due to their antibacterial activity [26].

We report herein on the morphological characteristics of the foams obtained by laser irradiation and on the accompanying laser induced photochemistry, assessed by on line monitoring of the laser induced fluorescence (LIF). We identify the laser conditions (pulse duration) at which foaming is produced and discuss the obtained results in reference to the material properties, particularly extinction coefficient and thermal parameters. The present study also aims at demonstrating the viability of the laser induced superficial microfoam structure for cell culture, made possible by overcoming the obstacle related with collapse of the prepared 2D polymer scaffold when in contact with water solution. Results of cell culture on microfoamed chitosan substrates prepared by single ns laser pulses are presented as an illustrative example of the possibility of the broader use of laser induced biopolymers foaming structures in biology.

2. Experimental

2.1 Sample preparation

Self standing films of the biopolymers chitosan and native high amylose corn starch, with a moisture of 11.40 % (both of them purchased from Aldrich), and a blend of the two materials were prepared by the method of solvent evaporation. Solutions of chitosan and chitosan/starch 50/50 wt. % in acetic acid 0.4 M (heating up to ca. 100 ºC in the case of the blend), and starch in boiling water were prepared in the concentrations listed in Table 1 and poured on Petri dishes with a diameter of 8.5 cm. The thicknesses of the resulting films are also reported in Table 1. The estimated surface roughness is in

the range of a few nanometres as determined by Atomic Force Microscopy (AFM) measurements. The mean roughness values (R_a) are also listed in Table 1, and represent the arithmetic average of the deviations from the centre plane of the sample. Each R_a value corresponds to the average of three independent measurements in different locations of the film. The UV-Vis absorption spectra of films of the above materials prepared by casting on quartz plates were measured with a UV-Vis-NIR-3600 Shimadzu spectrophotometer. Table 1 displays too the calculated linear extinction coefficients for the laser irradiation wavelengths of 213 and 248 nm, together with relevant material properties. As concerning the preparation of samples for cell culture, chitosan solutions in acetic acid were also casted on quartz plates and overnight dried.

2.2 Sample irradiation and characterization

Three laser systems delivering UV pulses of different duration in the ns to the fs range were used to irradiate the biopolymer films in ambient atmosphere and at normal incidence. These are a KrF excimer laser (Lambda-Physik Compex 210i, 248 nm, 20 ns FWHM), a Nd:YAG laser (EKSPLA SL-312, fifth harmonic at 213 nm, 150 ps FWHM) and a hybrid excimer-dye laser (248 nm, 500 fs FWHM). With each system, a series of spots was created in the different biopolymer samples by delivering a single laser pulse through a focusing lens at increasing fluences up to 2800 mJ/cm^2.

For the irradiation of chitosan casted on quartz, the samples were translated so that single pulse laser irradiation (248 nm, 20 ns) was always performed on a "fresh" area of the film, resulting in an array of irradiated spots. The irradiated chitosan films were treated with ethanol (95 %) for three days prior to cell culture.

Following the methodology described in [27], LIF was employed to detect the fluorescence from the substrate and thus to assess the chemical modifications of the irradiated surface. Fluorescence of the irradiated areas was induced by excitation with

the same laser used for irradiation (at 248 or 213 nm). Low fluences, in the range of 7-10 mJ/cm^2, were employed to ensure that modification of the substrate by the probe beam is negligible. The delay between the pump and the probe laser pulses was fixed in several seconds and the induced emission was collected by an optical fibre oriented nearly perpendicularly to the sample at ca. 2 cm away from its surface. The emission was spectrally analyzed in a 0.20 m grating spectrograph and the spectra recorded on an ICCD camera (Andor iStar) interfaced to a computer. Cut off filters (> 290 nm) were used for blocking any probe beam scattered light. Fluorescence spectra were collected using a detection gate of 255 ns by accumulating 50 probe pulses in each irradiated spot of the sample.

Scanning electron microscopy (SEM) served to investigate the morphology of the irradiated areas. To that purpose the films were gold coated by sputtering and analyzed by a JEOL JSM-6390LV system.

2.3 Cell cultures

Mouse NIH/3T3 fibroblasts were cultured in Dulbecco's modified Eagle's medium (DMEM) supplemented with 10% fetal bovine serum (FBS), and 1% antibiotic solution (GIBCO, Invitrogen, Karlsruhe, Germany). Confluent cell layers were detached using 0.05% trypsin/EDTA (GIBCO, Invitrogen, Karlsruhe, Germany). Cell suspensions at the concentration of 10^5 cells/ml were transferred to quartz plates containing the biopolymer structured surfaces and cultured at 37 ^{o}C in a 5% CO_2 atmosphere for 3, 5 and 7 days. Cell culture was performed on both non laser-treated and on laser-treated areas of chitosan films.

In order to study the cell viability and proliferation on irradiated biopolymer surfaces, a Live–Dead Cell Staining Kit (BioVision) was used. The detailed assay protocol has been previously described [8]. Stained healthy cells can be visualized green while dead

cells appear yellow-red. In addition, the number of fibroblasts per mm^2 (cell density) was calculated for all irradiated and non-irradiated areas of chitosan films. The number of live cells was calculated as the average of at least three measurements for each type of surface. All data are expressed as the mean value ± one standard deviation. The Student's t-test was used to compare the significance levels ($p < 0.001$) between control and test values.

The morphologies of NIH/3T3 fibroblasts seeded on biopolymer surfaces were observed by SEM. After culture termination, the cells were washed with 0.1 M sodium cacodylate buffer (SCB) and incubated with SCB for 15 minutes. This step was repeated twice and was followed by fixation of cells for 1 hour using a 2% glutaraldehyde, 2% formaldehyde in 1% SCB buffer at 4 °C. Subsequently, all surfaces were washed twice (15 minutes each time) with 1% SCB at 4 °C, dehydrated through a graded ethanol series (from 10 to 100 %) and incubated for 15 minutes on 100 % dry ethanol. Prior to electron microscopy examination, the samples were coated with a 10 nm gold layer. SEM was performed on a JEOL 7000 field emission scanning electron microscope operating at an acceleration voltage of 10 kV.

3. Results

3.1. Morphology of irradiated areas

Irradiation of the biopolymer films with the three different laser systems resulted in morphological modifications that were studied by SEM. Table 2 indicates the modification thresholds that were determined by measuring the fluence at which changes of the otherwise extremely smooth surfaces (roughness values listed in Table 1) were observed by SEM. As shown in Table 2, both wavelength and pulse duration have an effect on the threshold values. The lowest damage thresholds are found at 213 nm due to the efficient biopolymer absorption at this wavelength (linear extinction

coefficients listed in Table 1). At 248 nm, the thresholds observed with short pulses of 500 fs are reduced with respect to those measured under ns irradiation at the same wavelength. This is ascribed to the enhanced laser-material coupling mediated by fs-pulse induced multiphoton absorption. It is also worth noticing that at 248 nm, the highest thresholds are found in chitosan which, at this wavelength, is the less absorbing material.

Following irradiation of chitosan with a single 248 nm, 20 ns pulse, swelling of the surface and formation of micrometer size pores on the swelled region (of about 5 μm thick) are observed well above the modification fluence threshold (Figure 1a, at 2240 mJ/cm^2). It should be stressed that before irradiation, the surface of the film is smooth, with typical roughness $R_a \leq 5$ nm (Table 1), whereas the roughness measured after irradiation is two orders of magnitude higher, around 300-400 nm. Inspection of the porous structure at higher magnification (Figure 1d) reveals, as observed before [11,18], that the pores are interconnected and display average diameters of around one micron. The nature of the morphological modification is different for starch and chitosan/starch blend (shown in Figures 1b,c for 1800-1900 mJ/cm^2). In those materials the superficial foamy porous structure does not develop even at the highest fluences employed and destruction and ablation of the surface develops at sufficiently high fluence over the modification threshold.

Upon irradiation at 213 nm with 150 ps pulses (Figure 2), similar behaviour as the one reported for 20 ns, 248 nm is observed, where chitosan stands out as the sole material in which a uniform foamy layer is formed on the surface of the irradiated area at fluences above 100 mJ/cm^2. Again in this case, the laser effect on starch and chitosan/starch films results in ablation and eventually disruption of the sample skin. Figure 2d displays at high magnification the inner structure of the damaged film.

Finally, the shorter pulses of 500 fs, 248 nm introduce a different tendency. In this case (Figure 3) all materials behave similarly under laser irradiation and a foamy superficial layer (about 3 μm thick) of interconnected pores is generated under laser action. The porous structures have average diameters of around 0.5 microns, somewhat smaller than those of the microvoids produced in chitosan with 20 ns pulses of the same wavelength.

3.2. Fluorescence probing of irradiated areas

LIF spectra were collected from the non-irradiated and irradiated areas of the films in order to assess structural or chemical changes induced on the polymeric materials. Figure 4 displays spectra acquired before and following irradiation of the films surface with a single 248 nm, 20 ns pulse.

Spectra of chitosan consist of a broad band centred at 445 nm with a shoulder at 470 nm (Figures 4a,c). Differently, spectra of starch, with a considerable lower fluorescence yield (Figures 4b,d), display two well distinct bands centred at 331 and 432 nm. While the fluorescence of chitosan could not be attributed to any specific fluorophore, the visible fluorescence of starch can be assigned to the transition from nonbonding, namely *n* electrons in the hetero-atom (O) of the ether linkage functional group (C-O-C) which is part of the six-membered ring structure in starch molecule, to the antibonding orbital σ^* [28]. It is also expected that the minor protein component of the starch material (less than 1 %) contributes to the two fluorescence bands around 331 and 432 nm by virtue of the emissions from the amino acid tyrosine and its dimeric species, dityrosine, with matching reported emissions [15]. The spectra of the chitosan/starch mixture (not shown) resembles to that of chitosan due to the higher fluorescence yield of this material as compared with starch.

Irradiation with 20 ns pulses of 248 nm, at fluences high enough to induce the change of superficial morphology, does not affect the spectral distribution of the probed fluorescence from the films of chitosan (Figure 4a) and of its blend with starch, though the intensity of the broad band varies considerably with the fluence of irradiation. In contrast, the spectra of the irradiated starch sample (Figure 4b) show a relative increase of the longer wavelength band centred at 432 nm. Spectra collected upon illumination with 213 nm, 150 ps and 248 nm, 500 fs probes of the non laser-treated biopolymer films are similar to those obtained with the 248 nm, 20 ns probe. Figure 4c,d shows the case of 248 nm, 500 fs irradiation. Again at the fluences used to induce morphological modifications on the films under these laser conditions, similar effects, as reported above for the case of 248 nm, 20 ns, are observed; i.e. LIF spectra of chitosan (Figure 4c) and of the blend with starch maintain their spectral shape while the longer wavelength band of starch experiences a relative intensity increase (Figure 4d). The only difference concerns the magnitude of these modifications, as, in fact, the overall intensity of the emissions remains practically unaffected by laser irradiation with the shortest pulses of 500 fs. This is an indication of the reduced extent of the photochemical or structural changes induced on the material when using ultrashort pulses.

Previous studies provide some clues about the nature of the changes reported as monitored by on line LIF. Bajer and Kaczmarek [29] have investigated the effects of UV lamp irradiation on biodegradable blends of chitosan and starch with different component ratios and observed the growth of a new absorption band at 300 nm as a result of exposure. The intensity of this band increased with the content of chitosan in the mixture; this effect was attributed to the rupture of glycosidic bonds with chain scission and formation of free radicals, which upon oxidation lead to the creation of

ketone, aldehyde and carboxylic functionalities. It is expected that UV laser exposure of chitosan and chitosan/starch films should also trigger competitive photochemical reactions that might be responsible for the observed modifications in the LIF spectra reported herein for these samples.

On the other hand, the relative increase of the band of starch at 432 nm with respect to the one at 331 nm resembles the effect noticed by Gaspard et al. upon irradiation of self-standing films of gelatine [13,16] with UV pulses of ns and fs duration. In gelatine the relative increase of the long wavelength fluorescence band, assigned to dityrosine, was attributed to the combined effect of surface temperature rise and structural modifications induced by foaming. Katsumata et al.[30] have reported a strong dependence of the intensity of the visible starch photoluminescence on the sample temperature. Therefore in starch, and in similarity with the case of gelatine, either temperature increase or structural variations related with laser induced foaming could be responsible for the observed spectral changes.

3.3 Cell adhesion and proliferation on the microfoam structured surfaces

In Figure 5a, SEM images of the irradiated chitosan film after three days of cell culture are presented. For this trial we used a chitosan sample irradiated at 248 nm, 20 ns, with a fluence of 2800 mJ/cm^2, a value where efficient foaming of the surface is induced. An array of irradiated spots was created via the translation of the chitosan sample, so that single pulse laser irradiation was always performed on a "fresh" area of the biopolymer film. It is shown that the cells do preferentially proliferate on the laser-irradiated areas of the biopolymer surface while non-irradiated areas (within the white dotted lines) are not colonized by cells. Figure 5b is a magnification of the irradiated chitosan area showing the cells on the laser induced foamed region.

The preferred adhesion of fibroblasts on modified chitosan spots was confirmed by the Live-Dead Staining Kit assays. Figure 6 represents an indicative optical microscopy image (a) as well as the fluorescence microscopy images (b, c) of fibroblasts cultivated on chitosan films for 5 days. The region inside the dotted circular line corresponds to the area of the laser induced foam structure that it is surrounded by the non laser-irradiated chitosan surface.

Fluorescence microscopy images 6b, c show the live (green stained) cells cultivated on the chitosan surface. The image of Figure 6b is focused on the non laser-irradiated region of the chitosan film (outside the dotted area), whereas the image of Figure 6c is focused on the irradiated one (inside the dotted area). Although cell culture has already been tested on porous chitosan [25], the images presented here indicate the viability and non toxicity of laser-irradiated chitosan films for cell culture. Our results also indicate that the antibacterial properties of chitosan [26] do not imply toxicity to mammalian cells and on the contrary, for materials to be used in tissue engineering applications, the antibacterial properties constitute a unique advantage.

By using the images, as those presented in Figure 6b,c it was possible to quantify the cell density. We measured the cell density, given in number of cells per mm^2, on non-irradiated and irradiated areas after 1, 3, 5 and 7 days. Results appear in Figure 7 which proves the preferential fibroblast growth on the foam structures.

Figure 8 illustrates the laser-irradiated area of a chitosan film (casted on quartz) following single pulse irradiation at 248 nm, 20 ns and 2800 mJ/cm^2 after three days of cell culture. In general fibroblasts detect their substrate using the filopodia and their movement is facilitated by lamellipodium formation. As observed in Figure 8, the presence of lamellipodia is evident, indicating the strong cell adhesion on the foam structured surfaces. Since chitosan do not bears the usual adhesion promoter peptides of

the natural matrix, the cell explores the surface and probably secretes its own protein layer providing the promoting properties. The improved adhesion to the laser-treated surface should be ascribed to the increased substrate roughness. Evidence of the effect of surface roughness on cell adhesion has been previously reported [31]; in fact higher superficial roughness supplies cells with extra attachment area and configures a more favorable landscape for cell filopodia and adhesion proteins to migrate.

4. Discussion

As mentioned, the laser induced temperature increase and the evolution of the pressure wave are responsible for the nucleation and bubble growth which cause the fibrillar structures or foam on the surface of the biopolymer films reported herein. Following the approach described in [11,17], we have estimated the degree of heating and the amplitude of the pressure wave under the conditions of this work. The material parameters used in the calculations are listed in Table 1.

Upon irradiation at 248 nm, 20 ns pulses, the temperature increase on the sample surface can be approximated by $\Delta T= \alpha F/\rho C_p$, where α is the extinction coefficient, ρ is the density, C_p the specific heat and F is the laser fluence. On the other hand, the amplitude of the photoacoustic stress [11] is estimated by $P_0 =\beta AF/C_p\alpha\tau_p^2$, where β is the thermal conductivity, A is the absorptivity (approximated to be around 1 [11]), and τ_p the pulse duration. The calculated values of ΔT and P_0 are given in Table 3.

Inspection of the values listed in Table 3 indicates that the amplitude of the pressure wave induced by 248 nm, 20 ns pulses is not significantly different for chitosan and starch; however, due to the lower absorption coefficient of quitosan at 248 nm, the increase of temperature in this material is around one order of magnitude lower than in

starch. Under these irradiation conditions, the strong, temporally confined heating caused by laser irradiation is accompanied by an intense cavitation stress field which enables bubble nucleation and growth [17] and that finally results in the observed superficial foaming (Figure 1a). The fact that a superficial foamy layer is not generated on the surface of the films of starch and of chitosan/starch blend, even if the pressure and temperature rises are high enough, (Figure 1b,c) is related with the different thermal properties of the materials, in particular their characteristic thermal transitions (i.e. glass transition and melting temperatures). The glass transition temperature of chitosan is around 140 ºC [32] and this material is in amorphous state at room temperature. However, starch is a semicrystalline polymer and its glass transition takes place at around room temperature, or even at lower temperatures when the moisture content is over 20 % [33]. The absence of laser induced microstructures in starch are ascribed to the restricted polymer dynamics below the melting point, since the crystalline phase constitutes a robust scaffold that supplies mechanical stability to the material.

The above expressions used for ΔT and P_0 are not applicable for estimating the magnitude of heating and photoacoustic stress in the fs pulse regime. When irradiating with ultrashort pulses, the chemical, photothermal and photomechanical effects induced on the material are connected to the generation of large free electron densities in the laser created plasma [11,13,34,35]. Free electrons are formed through laser induced breakdown in a process that largely involves multiphoton ionization. In fact, with ultrashort fs pulses, the highly effective multiphoton absorption explains why the induced morphological changes are well localized on the outer layer (of few μm) of the films.

The temperature increase reached in the irradiated volume following single laser pulse irradiation can be calculated in the fs regime by $\Delta T = \varepsilon / \rho C_p$ [34]. The plasma energy

density at the end of the pulse is given by $\varepsilon = \rho_{cr}(9/4)E_i$, ρ_{cr} being the critical electron density and E_i the molecular ionization potential. While it is difficult to establish a criterion for calculating ρ_{cr},[35], and although contribution of multiphoton absorption processes can not be disregarded, the temperature increase reached in the irradiated volume sample should be somehow higher in starch than in quitosan, largely due to the higher linear absorption coefficient of the former.

Also in the ultrashort pulse regime, the sudden heating of the substrate induces the generation and propagation of a thermoelastic wave. The characteristic wave propagation time through the heated volume is defined as $\tau_m = 1/\alpha c_s$, where c_s is the sound propagation velocity. Under fs irradiation, the condition for confinement of thermoelastic stress, $\tau_p/\tau_m < 1$, is well established (see calculated values in Table 1), thus photomechanical effects play a definitive role in the observed material modifications. The amplitude of the pressure wave in the fs regime can be estimated through the expression [17] $p_0 = \Gamma\alpha F$. The dimensionless Grüneisen coefficient Γ is related to the material properties by $\Gamma = c_s^2\beta/C_p$, where β is the thermal expansion coefficient. Estimated values of p_0 for irradiation with 248 nm, 500 fs pulses are shown in Table 3. It is observed that the amplitude of the pressure wave is higher in the fs than in the ns regime (assuming equal irradiation fluences). Under fs irradiation, foaming is observed in all types of materials studied and the differences observed upon irradiation with 20 ns pulses are not evident any more. This is due to the shorter thermal diffusion length (Table 1) and additionally to the large laser intensities involved which promote multiphoton absorption and ionization as coupling channels of laser light with the outer film layers. Thus fs irradiation becomes a tool for the preparation of porous substrates with controlled dimensions in a wide range of biodegradable, biocompatible materials

with different characteristics because of the strong spatial confinement of temperature and pressure increase.

The SEM images of the laser-irradiated chitosan films constitute a strong evidence for the efficacy of single pulse laser induced superficial microfoaming of biopolymers in biological applications. The cells seem to preferentially select the microfoam structure created on the laser-treated areas of the chitosan film against the non-irradiated biopolymer areas. The laser foamed chitosan substrate provides an example of a biocompatible porous substrate to be exploited in biomedical applications. However, it is left to be clarified why the laser-irradiated chitosan films have to be treated with ethanol prior to cell culture. The authors ascribe this requisite to the laser induced photochemical changes on the chitosan surface following UV irradiation.

5. Conclusions

Irradiation in air of self-standing films of chitosan, starch and their blend with single laser pulses of 248 nm, 500 fs yields a porous, foamy superficial layer with submicrometric dimensions on the film surface. Upon UV irradiation with longer pulses (213 nm, 150 ps and 248 nm, 20 ns), this type of superficial morphology develops only in the case of chitosan. Using ultrashort fs pulses, the extent of material induced photochemical and structural modifications is reduced, as witnessed by on line laser induced fluorescence monitoring of the sample. These differences are related to the mechanisms operating under the different pulse temporal domains and to the material properties, particularly extinction coefficient and thermal phase transitions. Upon fs irradiation the strong spatial confinement of temperature and pressure increase drive the nucleation and growth of bubbles, finally leading to the observed superficial fibrillar structures or foam in all of the studied materials. The results presented show the control

capabilities of ultrashort laser pulses in obtaining porous substrates with submicrometric dimensions in biocompatible, biodegradable substrates and confirm that laser induced foam structures on biopolymer films are good prospect candidates for biological applications. Work is in progress, regarding cell culture on the substrates foamed under the different laser conditions of this work, in order to assess the effect of the various chemical characteristic of the substrate and of the morphological surface features, including pore size.

Acknowledgements

Funding from Ministry of Science and Innovation of Spain (MICINN) under Project CTQ2010-15680. E.R., M.O. and M.S. gratefully acknowledge Juan de la Cierva, CONSOLIDER CSD2007-00058, and Geomateriales (CAM, S2009/Mat-1629) Programs for contracts. The research leading to these results has received support from the access activities of the EC FP7-Infrastructures-2007 Project "Laserlab-Europe II" (Grant Agreement No: 212025) operating at the Ultraviolet Laser Facility, IESL-FORTH. A. Manousaki is acknowledged for SEM measurements.

References

[1] M. Oujja, S. Pérez, E. Fadeeva, J. Koch, B.N. Chichkov, M. Castillejo, Appl. Phys. Lett. 95 (2009) 263703.

[2] H. Jiankang, L. Dichen, L. Yaxiong, Y. Bo, L. Bingheng, L. Qin, Polymer 48 (2007) 4578.

[3] J.G. Fernandez, C.A. Mills, J. Samitier, Small 5 (2009) 614.

[4] S. Lazare, in M.M. Elnashar (Ed.), Biopolymers, Sciyo: Croatia, 2010, p.109.

[5] W.-C. Hsieh, C.-P. Chang, S.-M. Lin, Colloids Surf. B: Biointerfaces 57 (2007) 250.

[6] S. Psycharakis, A. Tosca, V. Melissinaki, A. Giakoumaki, A. Ranella, Biomed. Mater. 6 (2011) 045008.

[7] N. Koufaki, A. Ranella, K. Aifantis, M. Barberoglou, S. Psycharakis, C. Fotakis, E. Stratakis, Biofabrication 3 (2011) 045004.

[8] A. Ranella, M. Barberoglou, S. Bakogianni; C. Fotakis; E. Stratakis, Acta Biomaterialia 6 (2010) 2711.

[9] E. Stratakis, A. Ranella, M. Farsari, C. Fotakis, Progress in Quantum Electronics 33 (2009) 127.

[10] E. Stratakis, A. Ranella, C. Fotakis, Biomicrofluidics 5 (2011) 013411.

[11] S. Lazare, V. Tokarev, A. Sionkowska, M. Wisniewski, Appl. Phys. A 81 (2005) 465.

[12] E. Rebollar, G. Bounos, M. Oujja, S. Georgiou, M. Castillejo, J. Phys. Chem. B 110 (2006) 16452.

[13] S. Gaspard, M. Oujja, R. de Nalda, C. Abrusci, F. Catalina, L. Bañares, S. Lazare, M. Castillejo, Appl. Surf. Sci. 254 (2007) 1179.

[14] S. Gaspard, M. Oujja, R. de Nalda, M. Castillejo, L. Bañares, S.Lazare, R. Bonneau, Appl. Phys. A 93 (2008) 209.

[15] S. Gaspard, M. Forster, C. Huber, C. Zafiu, G. Trettenhahn, W. Kautek, M. Castillejo, Phys. Chem. Chem. Phys. 10 (2008) 6174.

[16] S. Gaspard, M. Oujja, C. Abrusci, F. Catalina, S. Lazare, J.P. Desvergne, M. Castillejo, J. Photochem. Photobiol. A: Chem. 193 (2008) 187.

[17] S. Lazare, R. Bonneau, S. Gaspard, M. Oujja, R. de Nalda, M. Castillejo, A. Sionkowska, Appl. Phys. A 94 (2009) 719.

[18] S. Lazare, I. Elaboudi, M. Castillejo, A. Sionkowska, Appl. Phys. A 101 (2010) 215.

[19] M. Castillejo, M. Oujja, E. Rebollar, S. Gaspard, C. Abrusci, F. Catalina, S. Lazare, Proc. SPIE 6261 (2006) 62611L.

[20] S.C.M. Fernandes, C.S.R. Freire, A.J.D. Silvestre, C.P. Neto, A. Gandini, J. Desbriéres, S. Blanc, R.A.S. Ferreira, L.D. Carlos, Carbohydr. Polym. 78 (2009) 760.

[21] H.Yi, L.-Q.Wu, W.E. Bentley, R. Ghodssi, G.W. Rubloff, J.N. Culver, G.F.Payne, Biomacromolecules 6 (2005) 2881.

[22] A. Buleon, P. Colonna, V. Planchot, S. Ball, Int. J. Biol. Macromol. 23 (1998) 85.

[23] T. Bourtoom, IUFoST 2006, DOI: 10.1051/IUFoST:20060515.

[24] D. Yumin, X. Zuyong, L. Rong, Wuhan University Journal of Natural Sciences 2 (1997) 220.

[25] C. Tangsadthakun, S. Kanokpanont, N. Sanchavanakit, T. Banaprasert, S. Damrongsakkul, Journal of Metals, Materials and Minerals 16 (2006) 37.

[26] M. Zhai, L. Zhao, F. Yoshii, T. Kume, Carbohydr. Polym. 57 (2004) 83.

[27] G. Bounos, E. Rebollar, A. Selimis, N. Bityurin, M. Castillejo, S. Georgiou, J. Appl. Phys. 100 (2006) 114323.

[28] T. Katsumata, T. Suzuki, H. Aizawa, E. Matashige, J. Food Eng. 78 (2007) 588.

[29] D. Bajer, H. Kaczmarek, in M.M. Jaworska, R. Brzezinski S. Minami, H. Pospieszny, A.A.F. Roberts, S. Senel, V. Varlamov (Eds.), Progress on Chemistry and Application of Chitin and Its Derivatives, Polish Chitin Society: Lodz, Poland, 2010, p.17.

[30] T. Katsumata, H. Aizawa, M. Saito, S. Komuro, T. Morikawa, SICE-ICASE International Joint Conference 4109217 (2006) 1578.

[31] N. Saranwong, K. Inthanon, W. Wongkham, P. Wanichapichart, D. Suwannakachorn, L.D. Yu, Nucl. Instrum. Meth. Phys. Res. B 272 (2012) 386.

[32] Y. Dong, Y. Ruan, H. Wang, Y. Zhao, D. Bi, J. Appl. Polym. Sci. 93 (2004) 1553

[33] R.L. Shogren, Carbohydrate Polymers 19 (1992) 83.

[34] A. Vogel, J. Noack, G. Huttman, G. Paltauf, Appl. Phys. B 81 (2005) 1015.

[35] A. Vogel, N. Linz , S. Freidank, G. Paltauf, Phys. Rev. Lett. 100 (2008) 038102.

[36] Z.B. Maroulis, K.K. Shah, G.D. Saravacos, J. Food Sci. 56 (1991) 773.

[37] A.E. Drouzas, Z.B. Maroulis, V.T. Karanthanos, G.D. Saravacos, J. Food. Eng. 13 (1991) 91.

Table 1. Preparation conditions of the biopolymer films and physical constants. The linear extinction coefficients at 213 and 248 nm were determined by UV-Vis absorption spectroscopy.

Material	**Chitosan**	**Starch**
Concentration (g/L)	20	7.5
Thickness (μm)	180	100
Roughness, R_a (nm)	3 ± 2	5.0 ± 0.4
Extinction coefficient α_{213} (m^{-1})	$2.0x10^5$	$1.7x10^5$
Extinction coefficient α_{248} (m^{-1})	$0.4x10^5$	$1.5x10^5$
Density ρ (Kg/m^3)	$1.3x10^3$ [(a)]	$1.5x10^3$ [(b)]
Specific heat C_p (J/ Kg K)	$3.9x10^3$ [(a)]	$1.2x10^3$ [(c)]
Thermal conductivity κ (W/ m K)	0.39 [(a)]	0.11 [(c)]
Absorptivity A	1	
Thermal expansion coeff. β (K^{-1})	$2.6x10^{-4}$ [(d)]	
Thermal diffusivity $D= \kappa/C_p\rho$ (m^2/s)	$7.7x10^{-8}$	$6.1x10^{-8}$
Speed of sound c_s (m/s)	$1.5x10^3$	
Grüneisen coefficient $\Gamma=c_s^2\beta/ C_p$	0.15	0.49
Optical penetration length $l_a=1/\alpha$ (m) at 213 nm at 248 nm	 $5.0x10^{-6}$ $2.5x10^{-5}$	 $5.9x10^{-6}$ $6.7x10^{-6}$
Thermal diffusion length $l_T=(D\tau_p)^{1/2}$ (m) for τ_p = 20 ns for τ_p = 500 fs	 $3.9 x10^{-8}$ $2.0x10^{-10}$	 $3.5x10^{-8}$ $1.7x10^{-10}$
Pressure length $l_p= c_s\tau_p$ (m) for τ_p= 20 ns for τ_p = 500 fs	 $3.0 x10^{-5}$ $7.5 x10^{-10}$	
Heat relaxation time $\tau_T= l_a^2/D$ (s) at 213 nm at 248 nm	 $3.2 x10^{-4}$ $8.1 x10^{-3}$	 $5.7 x 10^{-4}$ $7.4 x 10^{-4}$
Propagation time of pressure wave through irradiated volume $\tau_m=1/\alpha c_s$ (s) at 213 nm at 248 nm	 $3.3 x10^{-9}$ $1.7x 10^{-8}$	 $3.9 x10^{-9}$ $4.4 x10^{-9}$

[(a)] From reference [17].

[(b)] From reference [36].

[(c)] From reference [37]

[(d)] From reference [11].

Table 2. Modification thresholds (in mJ/cm^2) of the biopolymer films under different laser irradiation conditions.

Material	**248 nm, 20 ns**	**213 nm, 150 ps**	**248 nm, 500 fs**
Chitosan	700	< 100	500
Starch	300	< 100	200
Chitosan/Starch	500	< 100	300

Table 3. Temperature increase and amplitude of pressure wave as a result of laser irradiation of biopolymer films.

	Chitosan	**Starch**
248 nm, 20 ns, 1 J/cm^2		
ΔT (K)	79	830
P_0 (N/m^2)	4.2×10^7	3.6×10^7
248 nm, 500 fs, 1 J/cm^2		
p_0 (N/m^2)	6.0×10^7	7.4×10^8

Figure captions

Figure 1. SEM images of biopolymer samples irradiated at 248 nm with 20 ns pulses at the indicated fluences.

Figure 2. SEM images of biopolymer samples irradiated at 213 nm with 150 ps pulses at the indicated fluences.

Figure 3. SEM images of biopolymer samples irradiated at 248 nm with 500 fs pulses at the indicated fluences.

Figure 4. LIF spectra (λ_{exc}= 248 nm) collected from non laser-treated (black) and after single pulse irradiation (grey) with the indicated fluences: at 248 nm, 20 ns of a) chitosan and b) starch; and at 248 nm, 500 fs of c) chitosan and d) starch.

Figure 5. SEM image of chitosan film irradiated with a single laser pulse at 248 nm, 20 ns, 2800 mJ/cm^2 following cell culture of 3 days a), and the same picture in a greater magnification b). While the irradiated areas show cell proliferation, the darker areas in a) within the white dotted lines have not been exposed to laser irradiation and are not colonized by cells.

Figure 6. Optical microscopy images of fibroblasts cultured on chitosan surface after 5 days of culture a). Fluorescence microscopy images of live (green) cells cultured on chitosan surface after 5 days of culture b) and c). The outlined region indicates the area of the laser induced foam structure surrounded by the non irradiated chitosan surface. The images in b) and c) are focused on the non-irradiated and on the foamed structure of chitosan areas respectively. The 100 μm size bar applies to all figures.

Figure 7. Cell density (number of cells per mm^2) on the single-pulsed KrF laser-irradiated chitosan surface compared with the corresponding to the non laser-treated

one, after 1, 3, 5 and 7 days of culture. All experiments were performed in triplicate and the cell density values represent mean values ± SD.

Figure 8. SEM image of the laser induced foaming on chitosan films following single pulse irradiation at 248 nm, 20 ns after cell culture of 3 days.

Figure 1

248 nm, 20 ns

a) Chitosan

2240 mJ/cm^2

b) Starch

1800 mJ/cm^2

c) Chitosan/Starch

1900 mJ/cm^2

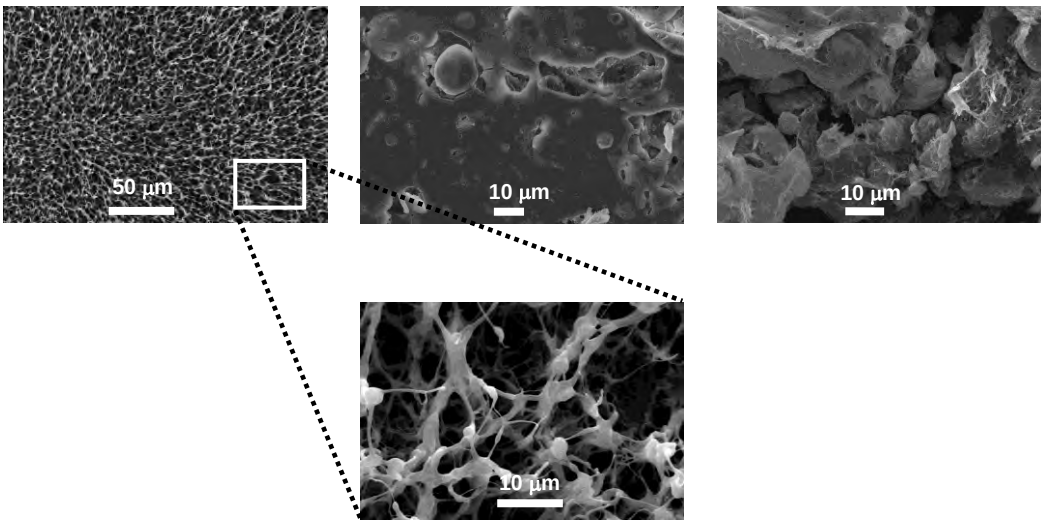

d) Chitosan

2240 mJ/cm^2

Figure 2

213 nm, 150 ps

a) Chitosan

880 mJ/cm^2

b) Starch

840 mJ/cm^2

c) Chitosan/Starch

840 mJ/cm^2

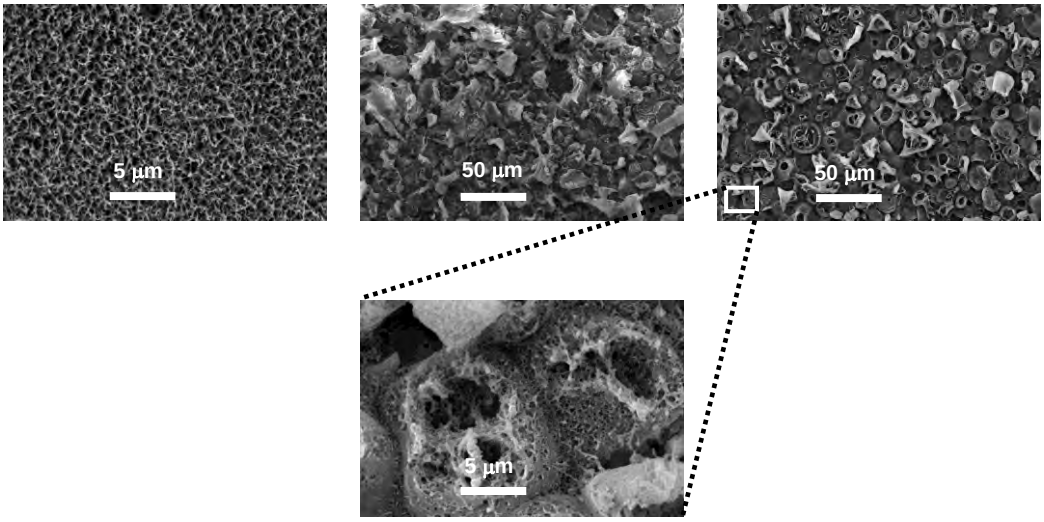

d) Chitosan/Starch

840 mJ/cm^2

Figure 3

248 nm, 500 fs

a) Chitosan

600 mJ/cm^2

b) Starch

600 mJ/cm^2

c) Chitosan/Starch

610 mJ/cm^2

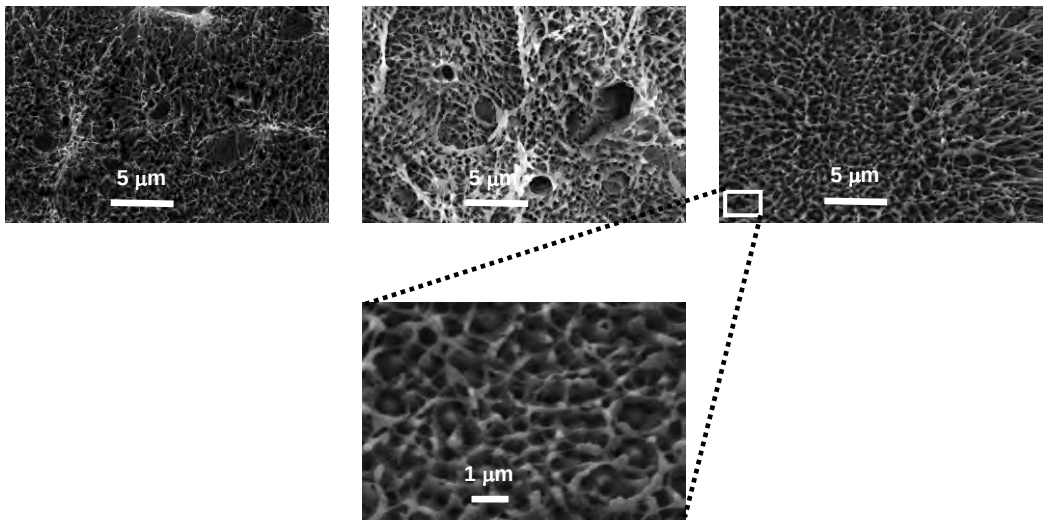

d) Chitosan/Starch

610 mJ/cm^2

Figure 4

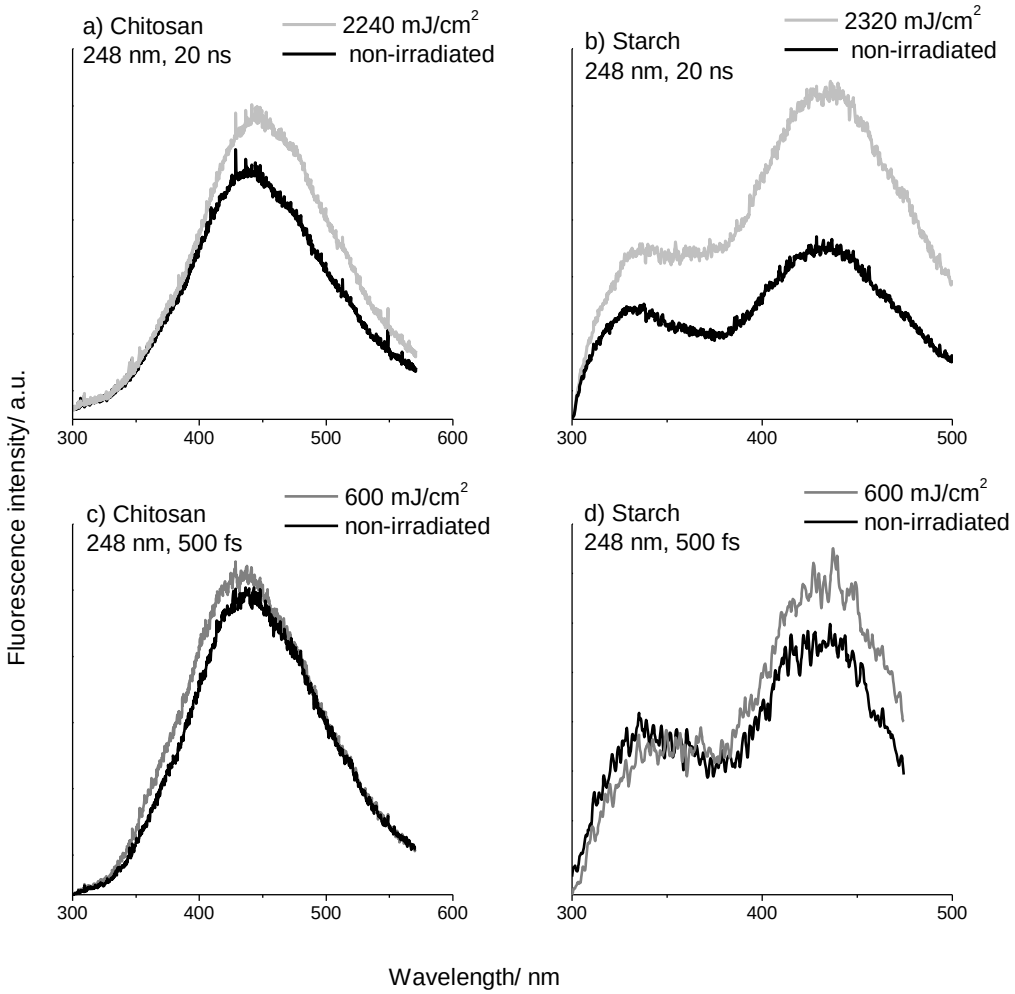
a) Chitosan
248 nm, 20 ns
2240 mJ/cm2
non-irradiated
b) Starch
248 nm, 20 ns
2320 mJ/cm2
non-irradiated
c) Chitosan
248 nm, 500 fs
600 mJ/cm2
non-irradiated
d) Starch
248 nm, 500 fs
600 mJ/cm2
non-irradiated
Fluorescence intensity/ a.u.
Wavelength/ nm
300
400
500
600

Figure 5

a) b)

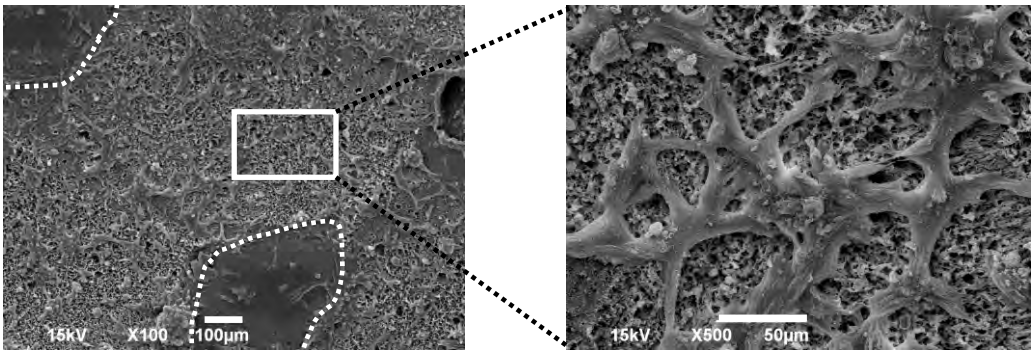

Figure 6

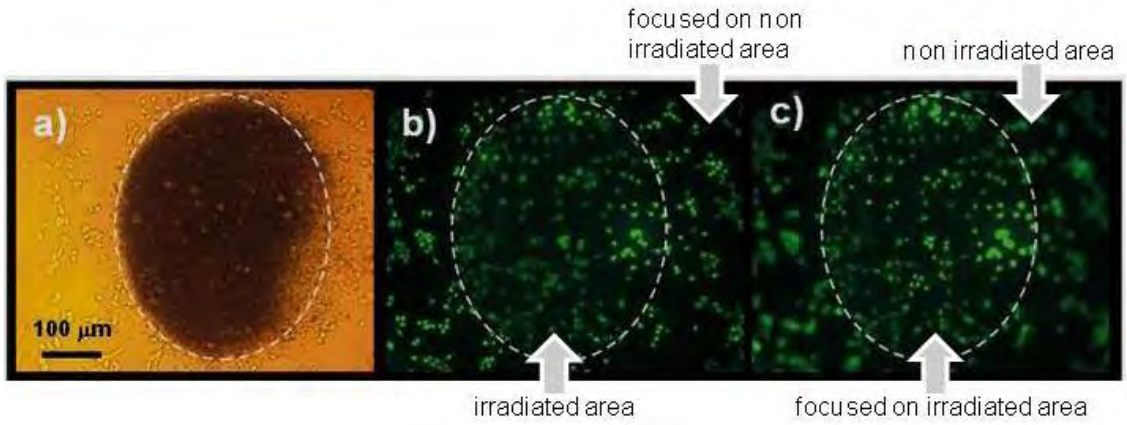
focused on non irradiated area
non irradiated area
a)
b)
c)
100 µm
irradiated area
focused on irradiated area

Figure 7

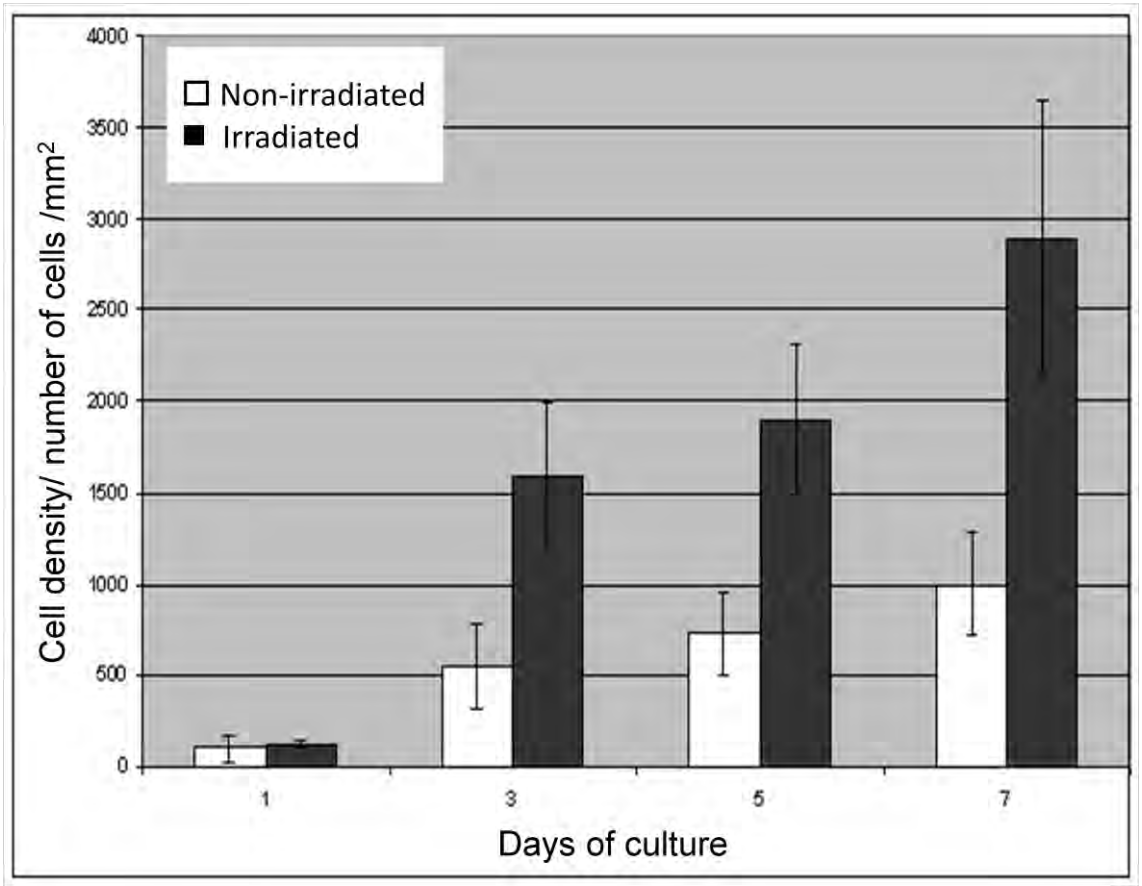
Non-irradiated
Irradiated
Cell density/ number of cells /mm2
4000
3500
3000
2500
2000
1500
1000
500
0
1
3
5
7
Days of culture

Figure 8

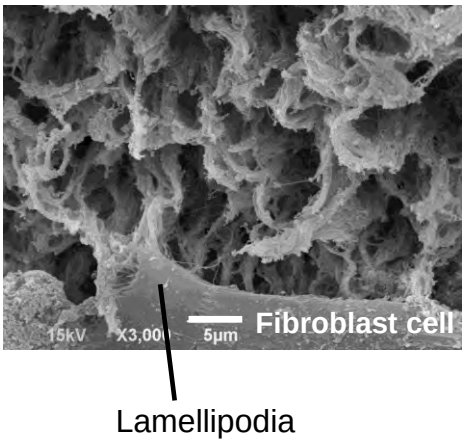

Graphical Abstract

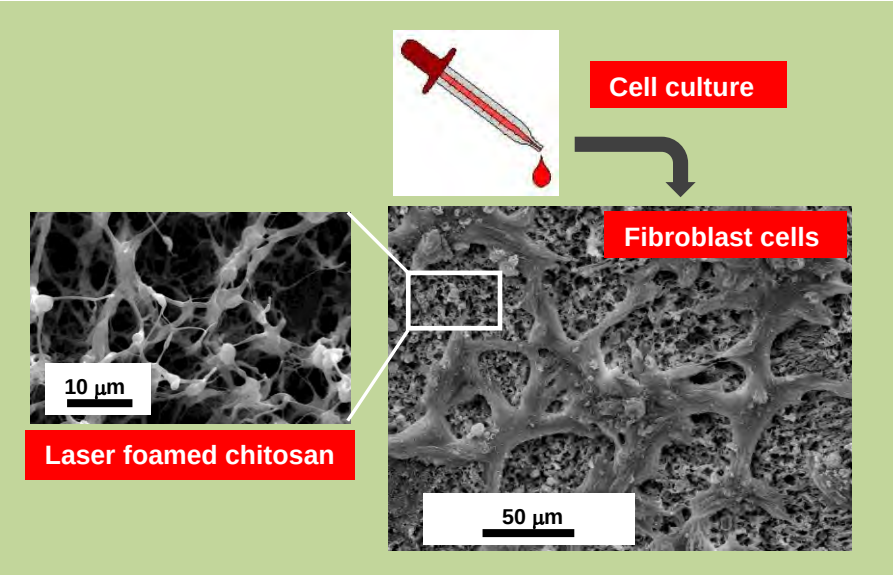

Highlights

- UV laser-induced superficial foaming in biopolymer films with fs, ps and ns pulses
- Reduction of photochemical and structural modifications by ultrashort fs irradiation
- Successful cell culture on laser-induced foam structure generated in chitosan

*Potential Reviewers

MINISTERIO
DE CIENCIA
E INNOVACIÓN

CSIC
CONSEJO SUPERIOR DE INVESTIGACIONES CIENTÍFICAS

INSTITUTO DE QUIMICA FISICA "ROCASOLANO"

We suggest three experts in the field to act as referees, as indicated in the web submission.

1) **Frederik Claeyssens**

The Kroto Research Institute
North Campus
University of Sheffield, Broad Lane, Sheffield, S3 7HQ, United Kingdom
Phone : 44 (0) 114 222 5513
Fax: 44 (0) 114 222 5943
e-mail: f.claeyssens@sheffield.ac.uk

2) **Roberto Pini**

Istituto di Fisica Applicata Nello Carrara
Viale delle Idee, 26 50019 Sesto Fiorentino, Italy
Phone : 055 522 5303-5304
Fax: 055 457 3302
e-mail: r.pini@ifac.cnr.it

3) **Maria Dinescu**

Plasma Radiation Physics National Institute for Lasers, NILPRP
Lasers Department
PO Box MG-16
Bucharest-Magurele RO-077125, Romania
Phone : 40 21 457 4470
Fax: 40 21 457 4243
e-mail: dinescum@ifin.nipne.ro

C/SERRANO, 119
28006 MADRID ESPAÑA
TEL.: 91 5619400
FAX: 91 5642431

Figure(s)

Click here to download Figure(s): Figure1.docx

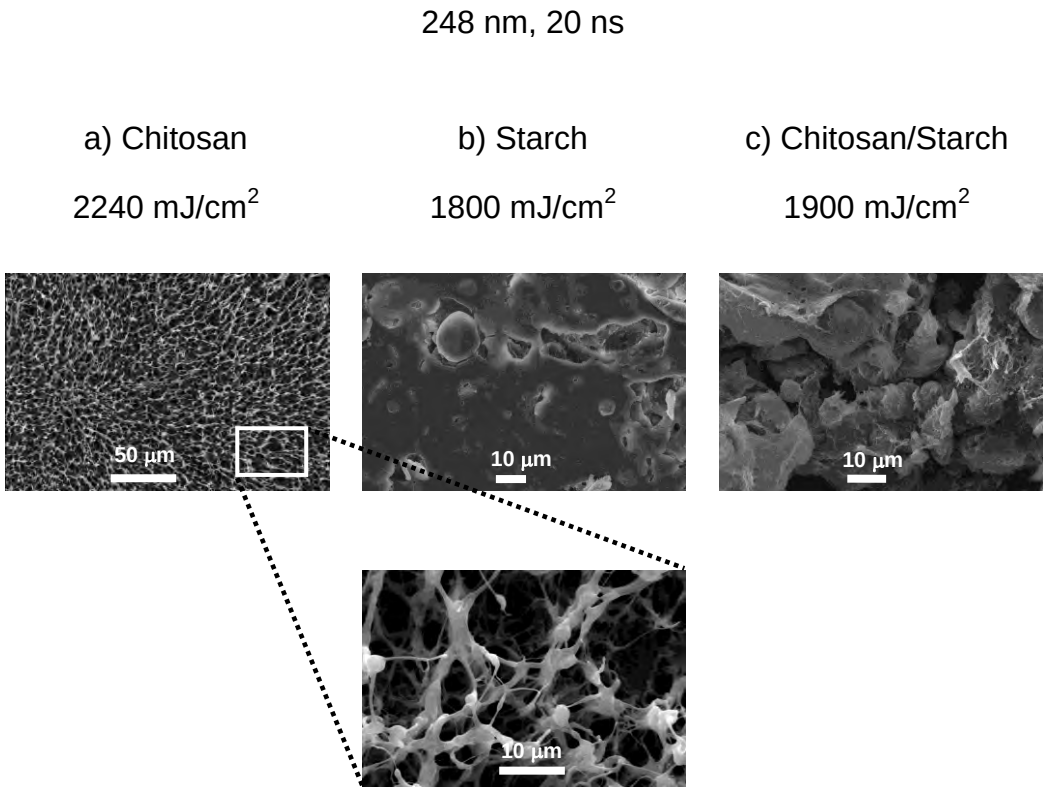

Figure(s)

Click here to download Figure(s): Figure2.docx

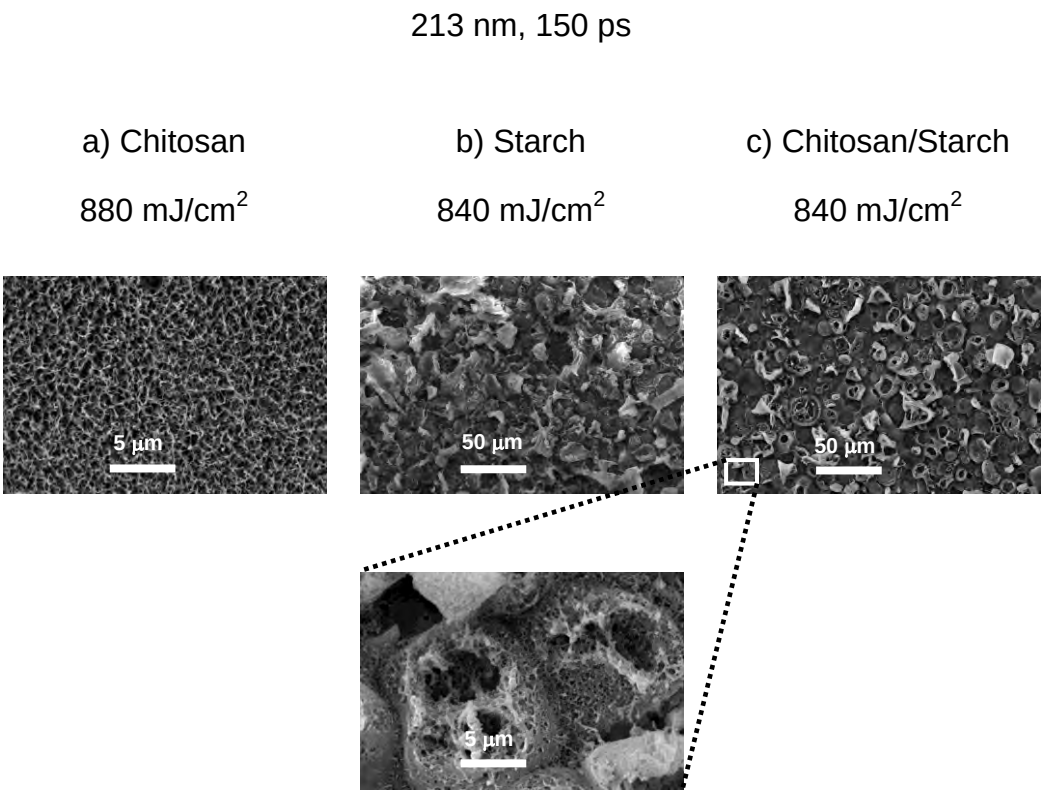

Figure(s)

Click here to download Figure(s): Figure3.docx

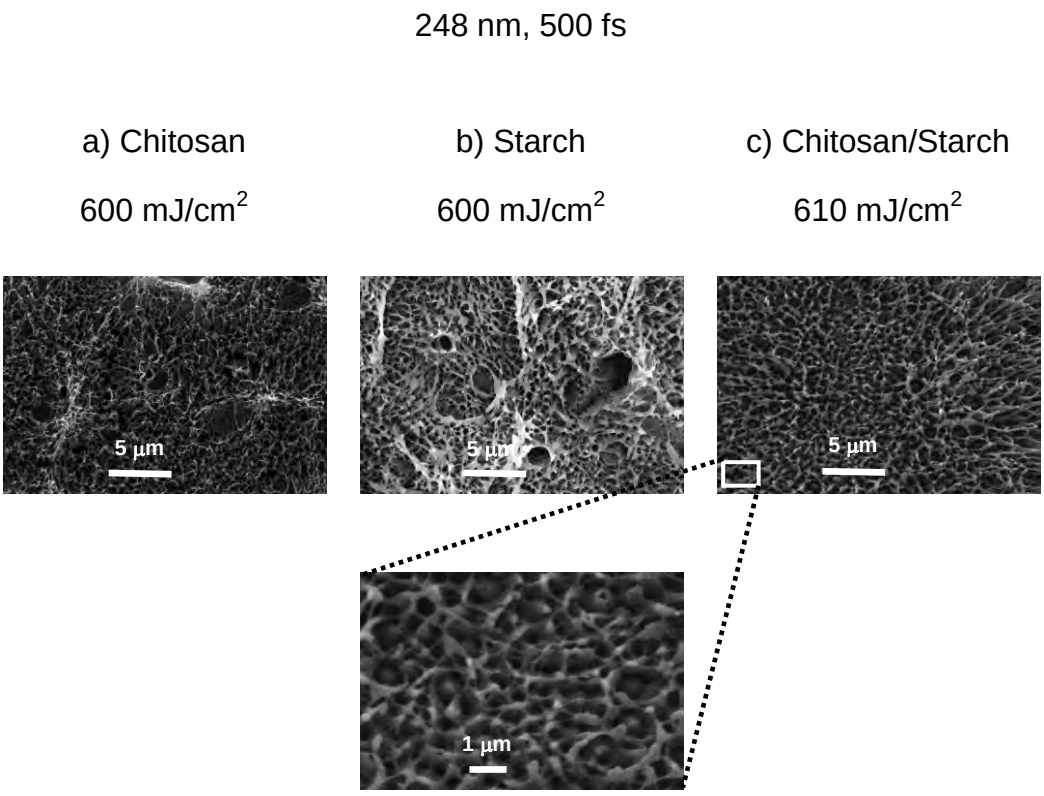

Figure(s)

Click here to download Figure(s): Figure4.docx

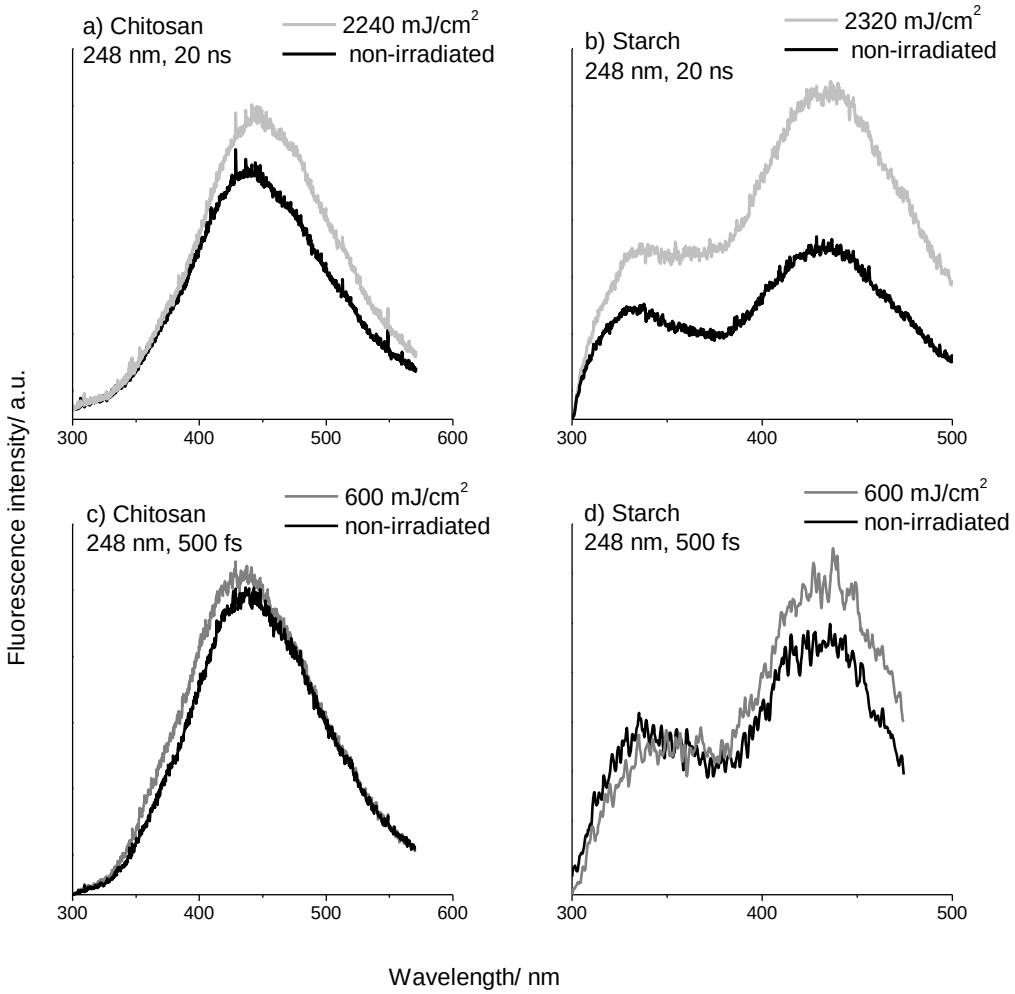

Figure(s)

Click here to download Figure(s): Figure 5.docx

Figure 5

a) b)

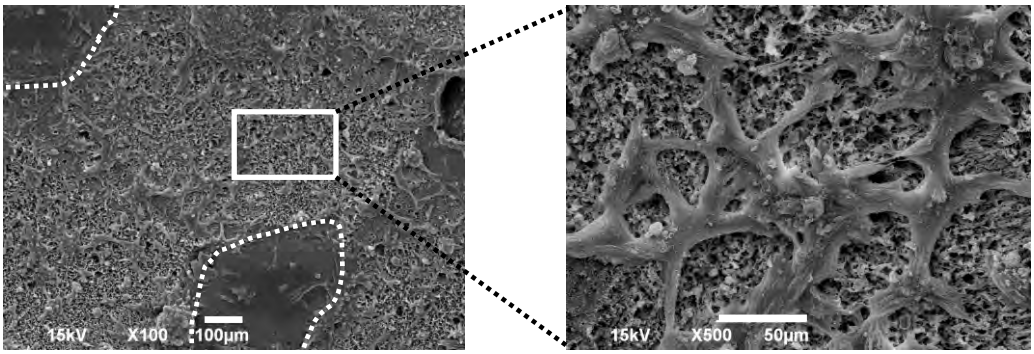

Figure(s)

Click here to download Figure(s): Figure 6.docx

Figure 6

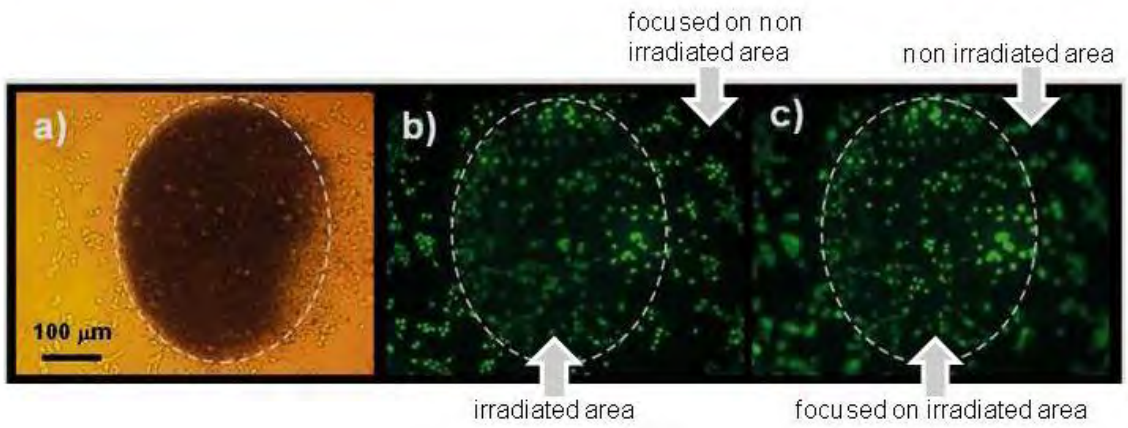

Figure(s)

Click here to download Figure(s): Figure7.docx

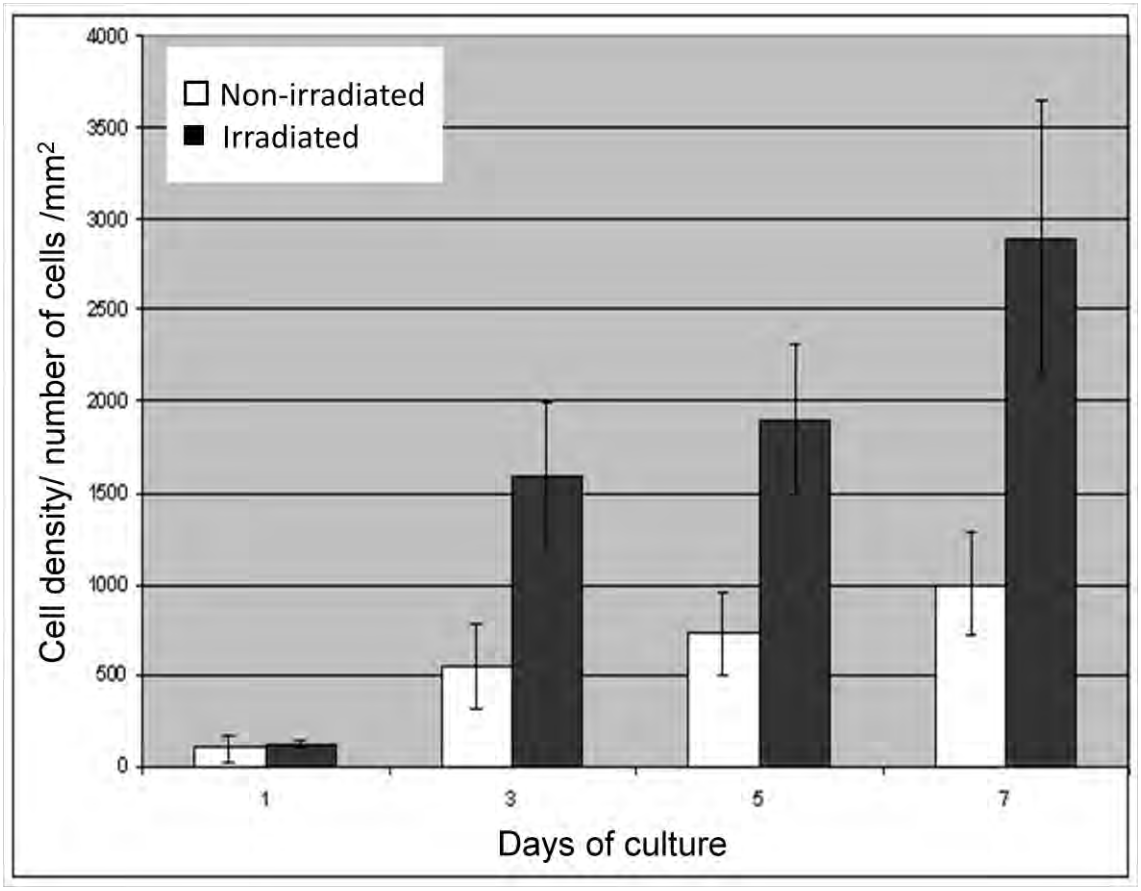

Figure(s)

Click here to download Figure(s): Figure8.docx

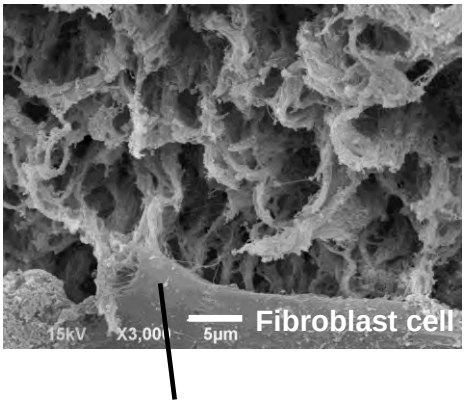

Table 1. Preparation conditions of the biopolymer films and physical constants. The linear extinction coefficients at 213 and 248 nm were determined by UV-Vis absorption spectroscopy.

Material	**Chitosan**	**Starch**
Concentration (g/L)	20	7.5
Thickness (μm)	180	100
Roughness, R_a (nm)	3 ± 2	5.0 ± 0.4
Extinction coefficient α_{213} (m^{-1})	$2.0x10^5$	$1.7x10^5$
Extinction coefficient α_{248} (m^{-1})	$0.4x10^5$	$1.5x10^5$
Density ρ (Kg/m^3)	$1.3x10^3$ [(a)]	$1.5x10^3$ [(b)]
Specific heat C_p (J/ Kg K)	$3.9x10^3$ [(a)]	$1.2x10^3$ [(c)]
Thermal conductivity κ (W/ m K)	0.39 [(a)]	0.11 [(c)]
Absorptivity A	1	
Thermal expansion coeff. β (K^{-1})	$2.6x10^{-4}$ [(d)]	
Thermal diffusivity $D= \kappa/C_p\rho$ (m^2/s)	$7.7x10^{-8}$	$6.1x10^{-8}$
Speed of sound c_s (m/s)	$1.5x10^3$	
Grüneisen coefficient $\Gamma=c_s^2\beta/ C_p$	0.15	0.49
Optical penetration length $l_a=1/\alpha$ (m) at 213 nm at 248 nm	 $5.0x10^{-6}$ $2.5x10^{-5}$	 $5.9x10^{-6}$ $6.7x10^{-6}$
Thermal diffusion length $l_T=(D\tau_p)^{1/2}$ (m) for τ_p = 20 ns for τ_p = 500 fs	 $3.9 x10^{-8}$ $2.0x10^{-10}$	 $3.5x10^{-8}$ $1.7x10^{-10}$
Pressure length $l_p= c_s\tau_p$ (m) for τ_p= 20 ns for τ_p = 500 fs	 $3.0 x10^{-5}$ $7.5 x10^{-10}$	
Heat relaxation time $\tau_T= l_a^2/D$ (s) at 213 nm at 248 nm	 $3.2 x10^{-4}$ $8.1 x10^{-3}$	 $5.7 x 10^{-4}$ $7.4 x 10^{-4}$
Propagation time of pressure wave through irradiated volume $\tau_m=1/\alpha c_s$ (s) at 213 nm at 248 nm	 $3.3 x10^{-9}$ $1.7x 10^{-8}$	 $3.9 x10^{-9}$ $4.4 x10^{-9}$

[(a)] From reference [17].

[(b)] From reference [36].

[(c)] From reference [37].

[(d)] From reference [11].

Table 2. Modification thresholds (in mJ/cm^2) of the biopolymer films under different laser irradiation conditions.

Material	**248 nm, 20 ns**	**213 nm, 150 ps**	**248 nm, 500 fs**
Chitosan	700	< 100	500
Starch	300	< 100	200
Chitosan/Starch	500	< 100	300

Table 3. Temperature increase and amplitude of pressure wave as a result of laser irradiation of biopolymer films.

	Chitosan	**Starch**
248 nm, 20 ns, 1 J/cm^2		
ΔT (K)	79	830
P_0 (N/m^2)	4.2x10^7	3.6 x10^7
248 nm, 500 fs, 1 J/cm^2		
p_0 (N/m^2)	6.0x10^7	7.4x10^8